

# Indoor To Indoor And Indoor To Outdoor Millimeter Wave Propagation Channel Simulations At 26 Ghz, 28 Ghz And 60 Ghz For 5G Mobile Networks

W. Manan, H. Obeidat, A. Al-Abdullah, R. Abd-Alhameed and F. Hu

*School of Engineering and Computer Science, Faculty of Engineering and Informatics*

*University of Bradford, Bradford, UK*

*Corresponding author: W. Manan*

---

## ABSTRACT

*In this paper the characteristics of LOS and NLOS propagations channels are intensively investigated under three mm wave frequencies; 26GHz, 28GHz and 60GHz for vertical polarized omnidirectional antenna. The simulation data achieved from the 3D shooting and bouncing Ray (SBR) tracer based on the effects of frequency dependent electrical properties of building materials and has been observed that signal is much affected by the nature of building materials and frequencies for line of sight and non-line of sight.*

**KEYWORD:** 5G, Line of Sight (LOS), Non-LOS (NLOS), Delay spread, path loss.

---

Date of Submission: 10-03-2018

Date of acceptance: 26-03-2018

---

## I. INTRODUCTION

A number of changes planned for 5G networks, is the extension into high frequencies in the wave spectrum, the increasing demands of high speed data and multimedia services, need to accurately predict multipath effects of indoor environments [1]. To support highly increasing traffic capacity and high data rates, the next generation mobile network (5G) should extend the range of frequency spectrum for mobile communication that is yet to be identified by the ITU-R [2]. The mm wave spectrum is the key enabling feature of next generation cellular system, for which the propagation channel models need to be predicted to enhance the design of the transceiver system.

In mobile radio propagation studies, the qualitative description of the environment are usually using terms rural, urban, dense urban and suburban [3]. Dense urban is the area defined tall buildings, commercial building areas and multi storey office blocks, while suburban is the area contains residential houses, flats, gardens and parks. Rural areas are generally defined as with scattered buildings and agricultural fields and forests. The average signal level in suburban and rural areas is better because of the environmental effect, so the signal variation in urban areas have been discussed so far [4]. In urban areas, there is no direct line of sight (LOS) between user equipment and base station (BS) antenna. There is a number of different paths because of reflection from a tall buildings, for which signal arrive at a mobile station (MS) through many paths and the received signal over each path has a random phase and amplitude [5]. Propagation models are designed by using deterministic approach and have become a preferred technique for channel propagation simulations. Deterministic is the model that can be performed through Maxwell's equation and by ray tracing techniques shooting and bouncing ray (SBR) [6].

At present, the current 4G systems provide a universal platform for broadband mobile services; however, mobile traffic is still growing at an unprecedented rate and the need for more sophisticated broadband services is pushing the limits on current standards to provide even tighter integration between wireless technologies and higher speeds. In [7] to meet the expected growth of wireless communications traffic, both efficient transmission schemes and additional spectrum allocations are needed. To support highly increasing traffic capacity and to enable the transmission bandwidths needed to support very high data rates, 5G will extend the range of frequencies used for mobile communication including indoor propagation environments [8-11]. The emerging technology 5G will use to enable mobile networks and devices to make better spectrum resources and will be expected to reach the mobile data to gigabits per second [12]. Recently the research work in propagation channel modelling is to understand the mechanisms of the propagation and the behaviour of the channel at frequencies above 6 GHz which had been published in [13-15].

Channel behaviour is identified by many parameters, in which the most important are path loss, received power, delay spread and angle of arrival. In this paper the propagation channel behaviour is examined

at three frequencies including: 26, 28 and 60 GHz using ray tracing commercial software called Wireless Insite. Channel modelling in [16] has used two frequencies: 28 and 73 GHz, however the study did not explain the propagation materials properties and different antenna radiation patterns at both transmitter and receiver.

In this paper the simulation environment for indoor-indoor propagation includes corridors in the 3<sup>rd</sup> floor Chesham building, University of Bradford, while for indoor-outdoor propagation includes route outside the Chesham building and a transmitter inside the building, which provides the comparisons of these metrics at 5.8, 26, 28 and 60GHz. The model includes the full description of buildings in terms of materials used where path loss, the received power and delay spread are evaluated. The organisation of this paper as follows: Section II summarized the investigated wireless channel characteristics, in section III simulation setup is presented, while in section IV simulation results are discussed, and finally conclusion is drawn in section V.

## II. WIRELESS CHANNEL CHARACTERISTICS

In this section the investigated propagation characteristics are introduced including: path loss model, received power and delay spread.

### A. Path loss model

Path loss is the reduction in power density of an electromagnetic wave when it propagates from transmitter to receiver. Due to differences in environments, it's difficult to make a general propagation model with detailed parameters; thus it's widely accepted to adopt a model that covers the main propagation aspects with reasonable results, this model The most simple and general path loss ( $PL$ ) is the  $n^{\text{th}}$  power law [17]:

$$PL(d)[dB] = PL(d_0) + 10n \log_{10}(d/d_0) + X_{\sigma}(1)$$

Where  $n$  is the path loss exponent which has different values as shown in table 1.  $d$  is the distance between the transmitter and the receiver,  $X_{\sigma}$  is Gaussian-distributed random variable with standard deviation  $\sigma$  dB for shadowing and  $PL(d_0)$  is the reference path loss, In order to exclude the near field effect of the measurements, power is measured in the far field region of the antenna at  $d_0$  (usually at 1 m) by applying Free space Friss formula or by empirical measurements [18]. reference path loss is given by[19]:

$$PL(d_0) = 20 \log_{10} \left( \frac{4\pi f}{c} \right) + 20 \log_{10}(d_0) - G_T - G_R \quad (2)$$

Where  $f, c, G_T$  and  $G_R$  are respectively: operating frequency, speed of light, transmitter gain and receiver gain.

**Table (1)** Path loss exponent values for different environments for (0.9 GHz and 1.9 GHz)[18, 20].

Environment	$n$
Free space	2
Urban macro cells	3.7-6.5
Urban microcells	2.7-3.5
Shaded urban microcells	3-5
Suburban	3-5
Indoor (single floor)	1.6-3.5
Indoor (Multiple floors)	2-6
Store	1.8-2.2
Factory	1.6-3.3
House	3

### B. Received Power

Received power is highly adopted in indoor environment for localization purposes [21-23]. The total received power can be obtained from the combination of the power for each ray path and the time average received power is given by [24] where  $N_p$  is the number of paths and  $P_i$  is the time average power for the  $i^{\text{th}}$  path,

$$P_R = \sum_{i=1}^{N_p} P_i \quad (3)$$

The effect of each path phase as [24] where  $\varphi_i$  is  $i^{\text{th}}$  ray phase in radian as shown in equation (4). While other models considers the paths coming from the same path to be combined with phase [25].

$$P_R = \left| \sum_{i=1}^{N_p} \sqrt{P_i} e^{-j\varphi_i} \right|^2 \quad (4)$$

### C. Delay Spread

Delay spread  $\sigma_{\tau}$  is defined as the square root of the second central moment which describes how the delays are spread with respect to the mean, although in many cases delay spread is similar to mean delay (first moment where each path contributes proportional to its power), however in cases where NLOS propagation is

dominant with large delay, the mean delay will provide a misleading indicator compared to the RMS delay. That is why  $\sigma_\tau$  is widely used as a delay spread metric [26].  $\sigma_\tau$  calculates the energy of power for each ray path reached in time and defined as a delay spread [27].

**Table(2)Median RMS delay spread in different environments[2]**

Frequency	Environment	Median RMS delay spread (ns)
1.9 GHz	House	70
	Office	100
	Commercial	150
2.625 GHz	Office	11
	Corridor	18.53
	Air cabin	11.89
	Factory	69.2
3.7 GHz	House	22
	Office	38
	Commercial	145
5.2 GHz	House	23
	Office	60
	Commercial	190
60 GHz	Office	1.77

$$\sigma_t = \sqrt{\frac{\sum_{t=1}^{N_p} (t_i - \bar{t})^2 P_i}{P_R}} \quad (5)$$

Where  $t_i$  is the arrival time while  $\bar{t}$  is the mean time of arrival. Table 2 presents typical Median RMS delay spread in different indoor environments.

#### D. Angle of arrival

In terms of spectral based techniques, AOA estimation methods can be classified to Beamforming techniques and Subspace techniques [28]. The idea behind beamforming is to let the array pattern to steer (using the weighting vector) to scan all possible angles, the angle which has the maximum corresponding power is considered as the AOA [29], two major algorithms are using beamforming concept in localization, Bartlett Beamformer and Capon minimum variance method [29]. Subspace techniques consider the effectiveness of the signal space and noise space, compared to beamforming techniques, subspace techniques show better performance and higher resolution estimation even with low SNR [28].

Antenna arrays can be used to detect angel of arrivals, direction of arrival is used for many application including beamforming, localization and detection [30], DOA requires the use of antenna arrays which is makes the technique more expensive and more power consumption compared to time of arrival (TOA) and received signal strength (RSS) [31]; however it requires less equipment's as only two Access Points are required to give a localization [32]. DOA is suitable in mediums with heterogeneous mediums (like water) where the velocity of waves will be different compared to those in free space, TOA and RSS will give an error in location estimation while DOA is less affected, that is why is used in biomedical localization specially in human body [30].

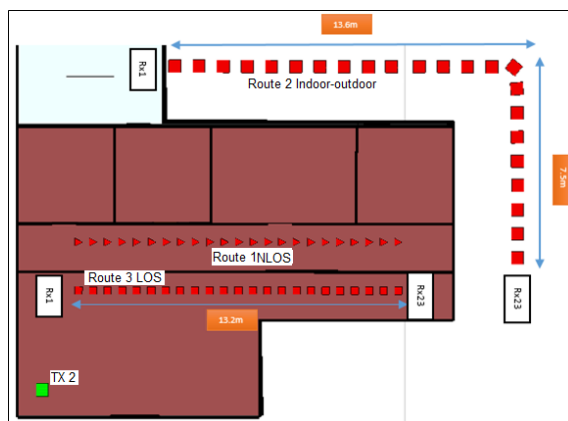
### III. SIMULATION SETUP

Simulations are conducted in the simulated environment of the third floor of Chesham building, University of Bradford. Where the transmitter is located on the third floor with three receiver routes representing LOS, NLOS and indoor to outdoor as shown in

Figure(1. The model was evaluated for three different scenarios such as same floor LOS 'Route 3', same floor NLOS 'Route 1' and indoor-outdoor 'Route 2', as shown in

Figure(1. The investigated frequencies include 26, 28 and 60 GHz (100MHz bandwidth) which are promising frequencies to be adopted for 5G networks.

The transmitter with vertically polarization omnidirectional antenna radiation pattern was fixed at 1m height from the floor. Both route 1 and route 3 had 23 receivers point each with 0.6 m separation from each other and 1 m height of the floor, each route examines different corridor of the building. Route 2 is located on the ground floor outside of the building with 23 receiver points 2 m in height from the city floor.



Figure(1):Floor layout with simulation routes and its dimensions.

Receiver’s sensitivity threshold was set to -160 dBm. It is to be noted that the receivers in triangular shape of Route 1 as shown in

Figure(1) is moving with an average velocity of 0.5 m/s, the properties of transmitter and receivers are described in table 3. The model completed by a detailed modelling using three types of walls: the outer concrete wall with 30cm thickness, layered dry wall with 12cm thickness and wooden wall. Two types of door used which includes wooden door (office doors) and, glass door and the type of window used, glass made window. The floor and ceiling is 3m above the floor and the second ceiling is simulated 2.5m above the floor with 3cm thick made of dielectric material.

Received power are varying for each frequency due to path loss and due to reflection and transmission losses of material where its electrical properties are function of frequency, in table 4 material properties values with frequency is presented according to the ITU recommendations [2]. The ray tracing settings are set as in table 5.

Table (3): Properties of transmitter and receiver antenna.

Properties	Transmitter antenna	Receiver Antenna
	Omnidirectional	Omnidirectional
Gain (dBi)	1.8	
Polarization	Vertical	Vertical
Waveform	Sinusoid	Sinusoid
Input Power (dBm)	23.0	-
E-Plane Half power bandwidth	90	-
Temperature (K)	293.00	293.00
VSWR	1.00	1.00
Receiver Threshold	-160.00	-160.00

Table (4) Material properties with frequency[2].

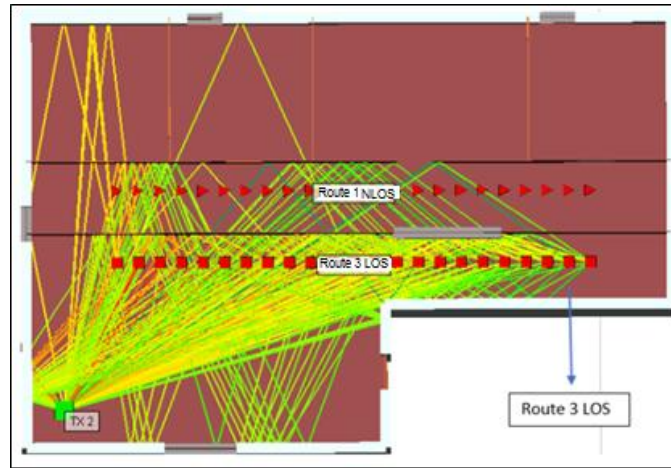
Frequency (GHz)	Concrete		Glass		Wood		Drywall	
	$\epsilon_r$	$\sigma$	$\epsilon_r$	$\sigma$	$\epsilon_r$	$\sigma$	$\epsilon_r$	$\sigma$
26	5.31	0.4557	6.27	0.1898	1.99	0.1544	2.94	0.1163
28	5.31	0.4838	6.27	0.2287	1.99	0.1672	2.94	0.1226
60	5.31	0.8967	6.27	0.5674	1.99	0.3784	2.94	0.2102

Table(5) Wireless Insite settings for the investigated scenario.

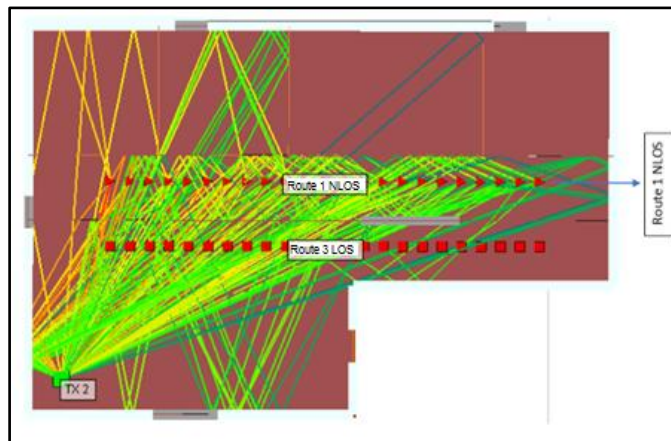
Property	Setting
Number of reflections	6
Number of transmissions	4
Number of diffractions	1
Number of reflections before first diffraction	3
Number of reflections after last diffraction	3
Number of reflections between diffractions	1
Number of transmission before first diffraction	2
Number of transmission after last diffraction	2
Number of transmission between diffractions	1
Ray tracing method	SBR
Propagation model	Full 3D

#### IV. RESULTS AND DISCUSSION

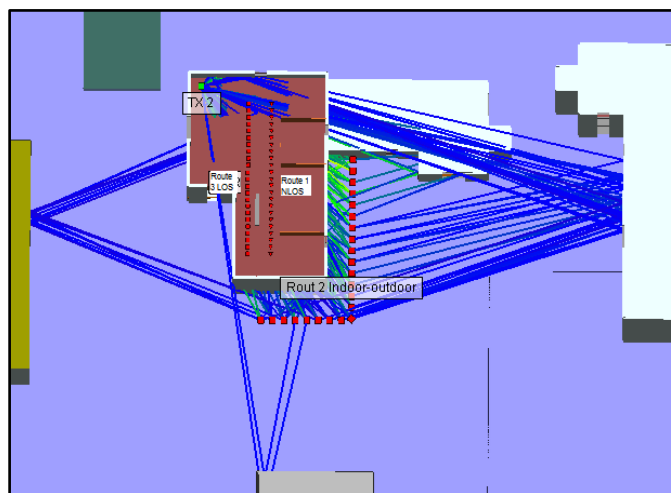
It is clear from the ray tracing in Figure(2 and Figure(3 that different materials interact with of rays differently. Some materials have less effect on signal attenuation compared to others. The low ratio of ray attenuation is from glass and layered dry wall. Comparatively for concrete walls, ray attenuations increase noticeably depending on wall thickness and the incident angle. In Figure(4 propagation paths for the indoor-outdoor scenario is presented, as expected longer paths tend to have lower signal strength.



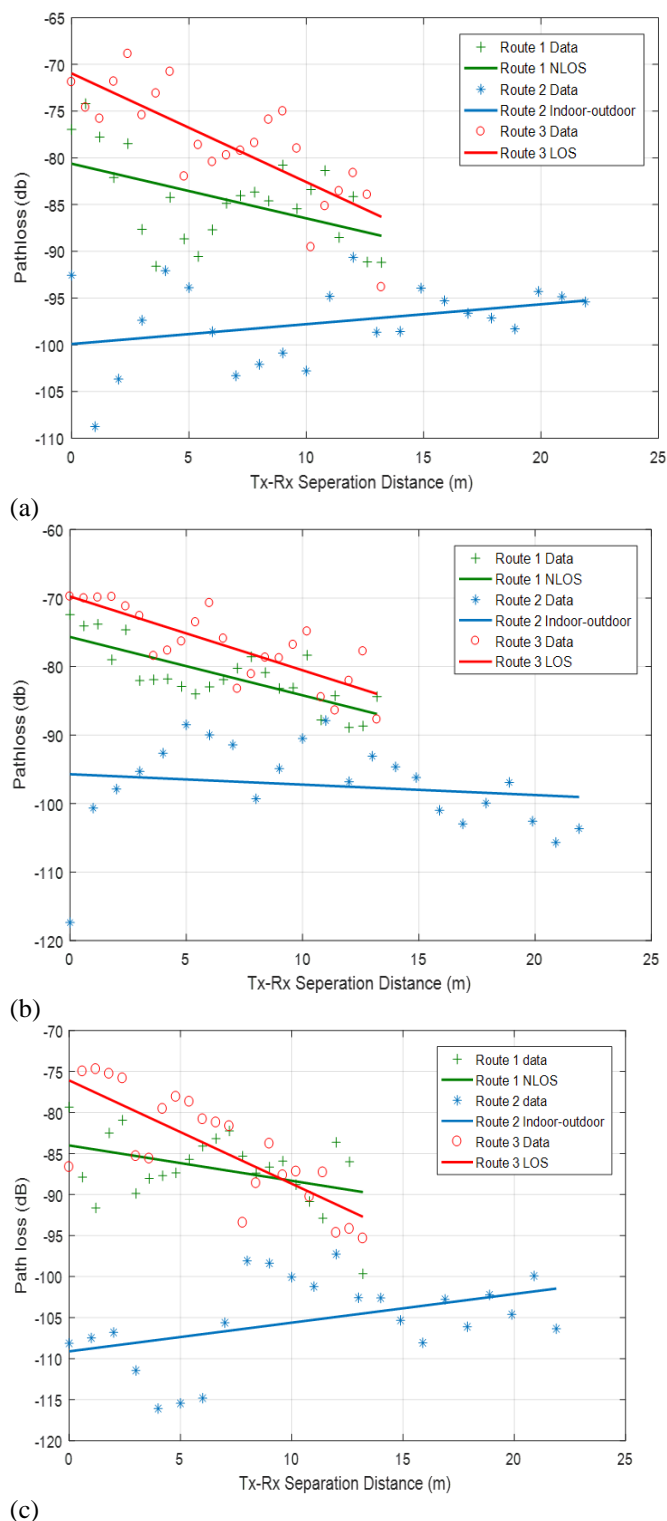
Figure(2): Route 3 (LOS) 3D SBR Propagation Model.



Figure(3): Route 1(NLOS) 3D SBR Propagation model.



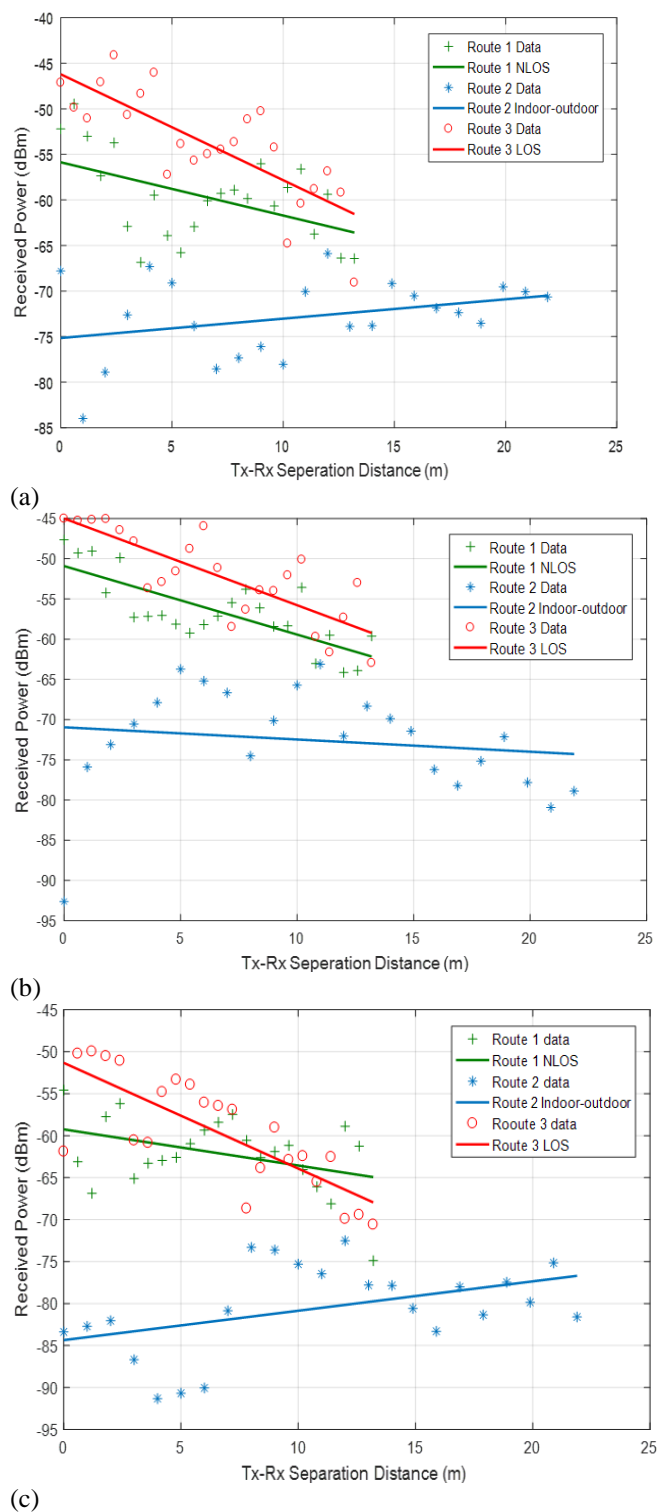
Figure(4): Route 2 (Indoor to outdoor) 3D SBR Propagation model.



**Figure(5):** Path loss vs Tx-Rx separation distance for LOS, NLOS, Indoor-outdoor at (a): 26, (b): 28 and (c): 60GHz

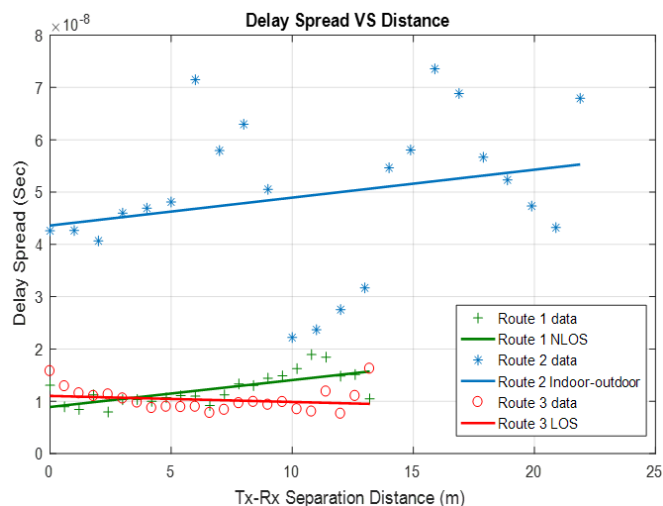
Figure(5) illustrates the path loss against the Tx-Rx separation distance. The path loss data in Figure(5) (a-c) is route 3 between -68 dB to -96 dB, route 1 -71 dB to -99 dB and route 2 is -89 dB to -116 dB. The path loss here increases because of the position of the receiver routes, distance between Tx-Rx and multipath channel propagation.

A simple slop channel model (solid lines) which represents polynomial fitting was adopted to summarise the results in Figure(5). It is shown in the simulated results that the path loss maximum variation (in dB) found for route 3, route 1, route 2 respectively are between  $\pm 4$ ,  $\pm 5$  and  $\pm 8$  at 26 GHz,  $\pm 4$ ,  $\pm 3$  and  $\pm 6$  at 28 GHz and GHz  $\pm 6$ ,  $\pm 7$  and  $\pm 8$  at 60.

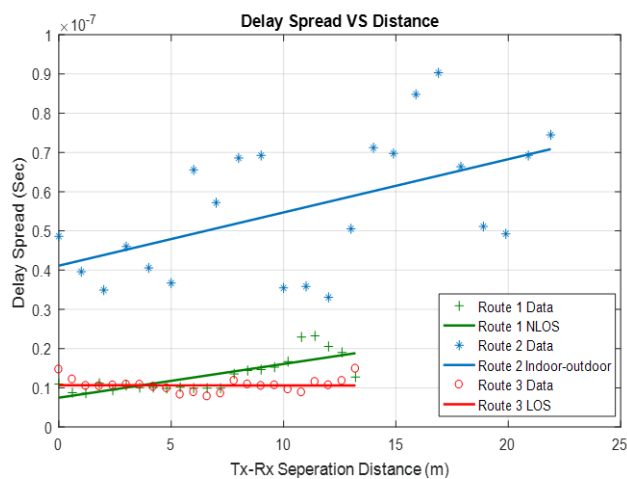


**Figure(6):** Received power vs Tx-Rx separation distance for LOS, NLOS, Indoor-outdoor at (a) 26 GHz, (b) 28 GHz and (c) 60GHz.

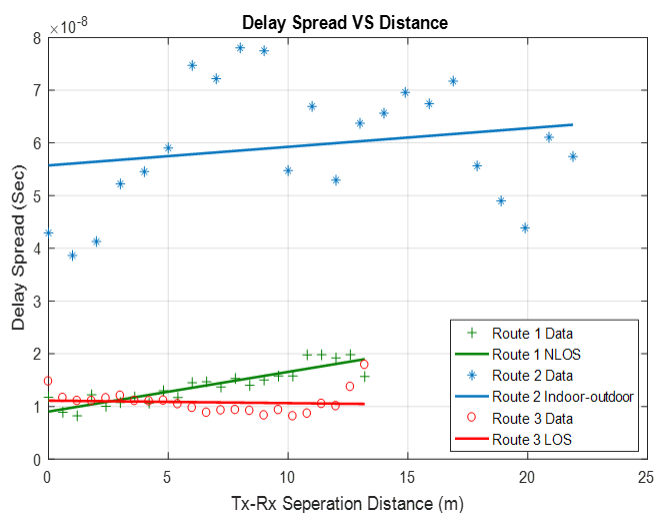
Figure(6) shows the received power at each receiver point against the Tx-Rx separation distance. The average result with curve fitting for route 3, the received power data in Figure(6) is between -44 dBm to -70dBm, route 1 -48 dBm to -75 dBm and for route 2 is -62 dBm to -92 dBm. The average power here at each receiver point is decreases because of the distance, nature of frequency and multipath channel propagation.



(a)



(b)



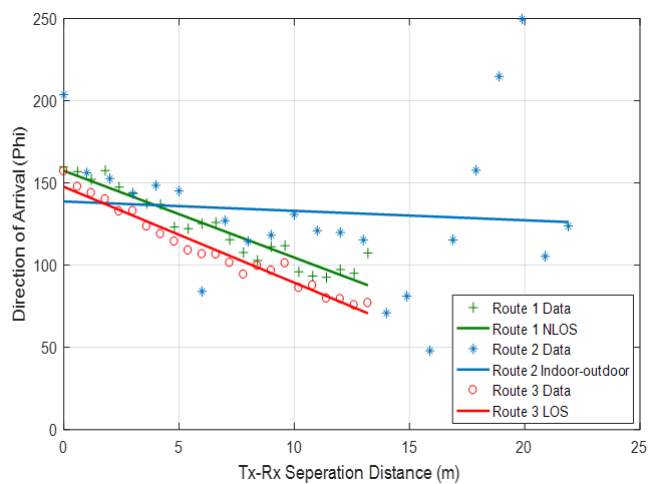
(c)

**Figure (7):** Delay Spread vs Tx-Rx separation distance for LOS, NLOS, Indoor-outdoor at (a) 26 GHz, (b) 28 GHz and (c) 60GHz.

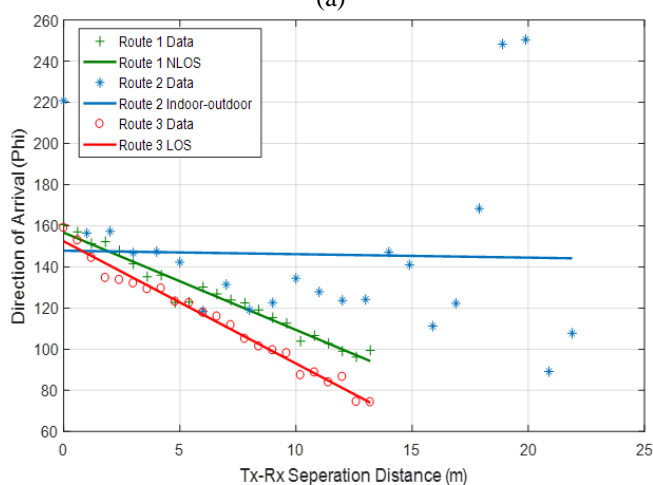
Figure (7) shows a comparison between the performance of the three different frequencies using omnidirectional antenna for route 3, route 1 and route 2. It can be observed that at 26GHz the delay spread is higher than at 28 GHz and 60GHz especially for route 2. The delay spread for route 2 is much higher as

compared to route 3 and 1 because of the height of the transmitter and large number of materials assumptions used between them. The initial rise is due to the position of the receivers with respect to the transmitter antenna.

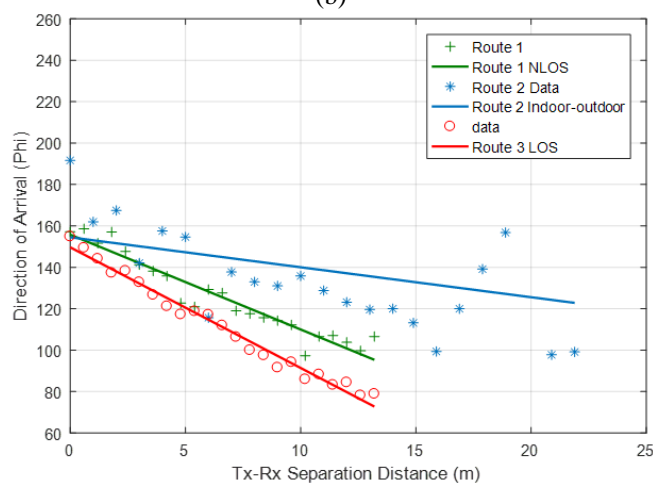
For LOS at higher separation distance the travel time of all multipath components are mostly the same, resulting much smaller delay spread between each receiver point. Figure shows a comparison between the mean direction of arrival of the examined frequencies using omnidirectional antenna for route 3, route 1 and route 2. Figure(8(a)) presents the arrival direction at 26 GHz in which the true angle found where the ray arrives at the receiver point in simulation is 70-160 degrees, 75-160 degrees and 80-160 degrees respectively. Followed the same procedure the direction of arrival for 28GHz and 60 GHz is found in Figure(8(b)) and Figure(8(c)).



(a)



(b)



(c)

**Figure(8):** Mean Direction of Arrival vs Tx-Rx Separation distance(m) for LOS, NLOS, Indoor-outdoor with linear fitting and at frequencies (a) 5.8GHz, (b) 26GHz, (c) 28GHz and (d) 60GHz.

## V. CONCLUSIONS

Indoor-indoor and indoor-outdoor including line of sight (LOS) and Non-line of sight (NLOS) propagation channel are investigated for three different mm wave spectrum. The effect of building materials, multipath effects and channel characteristics such as path loss, received power, direction of arrival and delay spread at separation distance in (m) from transmitter (Tx) to receiver (Rx) has been presented. It has been observed that signal is much more effected by concrete walls, also reacting differently for LOS and NLOS at each particularized frequency. Another important aspect is the position of the receivers, transmitter antenna directivity and the distance between TX-RX. The results shown that path loss behaves at higher frequency and due to the number of obstructions while the received power and delay spread decreases by increasing frequency.

## REFERENCES

- [1] K. Chandra, Z. Cao, T. M. Bruintjes, R. V. Prasad, G. Karagiannis, E. Tangdionga, *et al.*, "mCRAN: a radio access network architecture for 5G indoor communications," in *Communication Workshop (ICCW), 2015 IEEE International Conference on*, 2015, pp. 300-305.
- [2] I. T. U. ITU, "Propagation data and prediction methods for the planning of indoor radiocommunication systems and radio local area networks in the frequency range 900 MHz to 100 GHz," in *Recommendation ITU-R P.1238-7*, ed. Geneva: ITU, 2012.
- [3] L. W. Barclay, *Propagation of radiowaves* vol. 502: Iet, 2003.
- [4] R. Janaswamy, *Radiowave propagation and smart antennas for wireless communications*: Springer Science & Business Media, 2001.
- [5] M. V. S. Mr. ANIL KUMAR KODURI , Mr. M. KHALEEL ULLAH KHAN, ""Propagation Characteristics of a Mobile Radio Channel for Rural, Suburban and Urban Environments"," *IPASJ International Journal of Electronics & Communication (IJEC)*, vol. 2, 2014.
- [6] H. Ling, R.-C. Chou, and S.-W. Lee, "Shooting and bouncing rays: Calculating the RCS of an arbitrarily shaped cavity," *IEEE Transactions on Antennas and propagation*, vol. 37, pp. 194-205, 1989.
- [7] K. B. J. Medbo, K. Haneda , V. Hovinen, T. Imai, J. Järveläinen, T. Jämsä, ""Channel Modelling for the Fifth Generation Mobile Communications"," presented at the Antennas and Propagation (EuCAP), 2014 8th European Conference on, The Hague, Netherlands, 2014.
- [8] Z. Cao, X. Zhao, F. M. Soares, N. Tessema, and T. Koonen, "38-GHz Millimeter Wave Beam Steered Fiber Wireless Systems for 5G Indoor Coverage: Architectures, Devices and Links," *IEEE Journal of Quantum Electronics*, 2016.
- [9] M. K. Samimi and T. S. Rappaport, "Characterization of the 28 GHz millimeter-wave dense urban channel for future 5g mobile cellular," *Technical Report, TR 2014-001*, 2014.
- [10] G. R. Maccartney, T. S. Rappaport, S. Sun, and S. Deng, "Indoor Office Wideband Millimeter-Wave Propagation Measurements and Channel Models at 28 and 73 GHz for Ultra-Dense 5G Wireless Networks," *IEEE Access*, vol. 3, pp. 2388-2424, 2015.
- [11] A. A. AlAbdullah, N. Ali, H. Obeidat, R. A. Abd-Alhameed, and S. Jones, "Indoor millimetre-wave propagation channel simulations at 28, 39, 60 and 73 GHz for 5G wireless networks," presented at the Internet Technologies and Applications (ITA), Wrexham, United Kingdom, 2017.
- [12] S. Sun, G. R. MacCartney, and T. S. Rappaport, "Millimeter-wave distance-dependent large-scale propagation measurements and path loss models for outdoor and indoor 5G systems," in *Antennas and Propagation (EuCAP), 2016 10th European Conference on*, 2016, pp. 1-5.
- [13] M. K. S. Sijia Deng, Theodore S. Rappaport, ""28 GHz and 73 GHz millimeter-wave indoor propagation measurements and path loss models"," presented at the Communication Workshop (ICCW), 2015 IEEE International Conference on, London, UK, 2015.
- [14] T. S. R. Shu Sun, Rimma Mayzus, ""Millimeter Wave Mobile Communications for 5G Cellular: It Will Work!"," pp. 335 - 349, 2013.
- [15] T. S. R. Sundeep Rangan, Elza Erkip, ""Millimeter-Wave Cellular Wireless Networks: Potentials and Challenges"," vol. 102, 2014.
- [16] T. S. R. GEORGE R. MacCARTNEY, D SIJIA DENG, ""Indoor Office Wideband Millimeter-Wave Propagation Measurements and Channel Models at 28 and 73 GHz for Ultra-Dense 5G Wireless Networks," *SPECIAL SECTION ON ULTRA-DENSE CELLULAR NETWORKS*, vol. 3, 2015.
- [17] M. Lott and I. Forkel, "A multi-wall-and-floor model for indoor radio propagation," in *Vehicular Technology Conference, 2001. VTC 2001 Spring. IEEE VTS 53rd*, Rhodes, Greece, Greece, 2001, pp. 464-468.
- [18] T. S. Rappaport, *Wireless communications: principles and practice*, 2 edition ed. Upper Saddle River, NJ, USA: Prentice Hall, 2002.
- [19] S. Saunders and A. Aragón-Zavala, *Antennas and Propagation for Wireless Communication Systems: 2nd Edition*: John Wiley & Sons, 2007.
- [20] A. Goldsmith, *Wireless communications*: Cambridge university press, 2005.
- [21] H. A. Obeidat, Y. A. Dama, R. A. Abd-Alhameed, Y.-F. Hu, R. S. Qahwaji, J. M. Noras, *et al.*, "A Comparison between Vector Algorithm and CRSS Algorithms for Indoor Localization using Received Signal Strength," *The Applied Computational Electromagnetics Society (ACES)*, vol. 31, pp. 868-876, August 2016 2016.

- [22] H. Obeidat, W. Shuaieb, H. Alhassan, K. Samarah, M. Abousitta, R. Abd-Alhameed, *et al.*, "Location based services using received Signal Strength algorithms," in *Internet Technologies and Applications (ITA), 2015*, Wrexham, UK, 2015, pp. 411-413.
- [23] H. Obeidat, O. Obeidat, W. Shuaieb, A. Alabdullah, Y. Dama, M. Binmelha, *et al.*, "Performance Comparative Study Between Vector And ECOLOCATION Algorithms For Indoor Positioning," in *Internet Technologies and Applications (ITA), 2017*, Wrexham, UK, 2017, pp. 230-234.
- [24] R. A. Valenzuela, O. Landron, and D. Jacobs, "Estimating local mean signal strength of indoor multipath propagation," *IEEE transactions on vehicular technology*, vol. 46, pp. 203-212, 1997.
- [25] REMCOM, "Wireless InSite Reference Manual," 3.1.0 ed. State College, Pennsylvania: REMCOM, 2017.
- [26] J. S. Seybold, *Introduction to RF propagation*: John Wiley & Sons, 2005.
- [27] S. Salous, *Radio Propagation Measurement and Channel Modelling*: John Wiley & Sons, 2013.
- [28] J. Foutz, A. Spanias, and M. K. Banavar, "Narrowband direction of arrival estimation for antenna arrays," *Synthesis Lectures on Antennas*, vol. 3, pp. 1-76, 2008.
- [29] H. Krim and M. Viberg, "Two decades of array signal processing research: the parametric approach," *Signal Processing Magazine, IEEE*, vol. 13, pp. 67-94, 1996.
- [30] R. Zekavat and R. M. Buehrer, *Handbook of position location: Theory, practice and advances* vol. 27: John Wiley & Sons, 2011.
- [31] N. Patwari, J. N. Ash, S. Kyperountas, A. O. Hero III, R. L. Moses, and N. S. Correal, "Locating the nodes: cooperative localization in wireless sensor networks," *Signal Processing Magazine, IEEE*, vol. 22, pp. 54-69, 2005.
- [32] H.-C. Chen, T.-H. Lin, H. Kung, C.-K. Lin, and Y. Gwon, "Determining RF angle of arrival using COTS antenna arrays: a field evaluation," in *MILITARY COMMUNICATIONS CONFERENCE, 2012-MILCOM 2012*, 2012, pp. 1-6.

W. Manan. "Indoor To Indoor And Indoor To Outdoor Millimeter Wave Propagation Channel Simulations At 26 Ghz, 28 Ghz And 60 Ghz For 5G Mobile Networks " *The International Journal of Engineering and Science (IJES)* 7.3 (2018): 08-18